Plasmon localization, plasmon relaxation, and thermal transport in one-dimensional conductors

M. Bard,[1] I. V. Protopopov,[2,3] and A. D. Mirlin[1,4,5,3]

[1]*Institut für Nanotechnologie, Karlsruhe Institute of Technology, 76021 Karlsruhe, Germany*
[2]*Department of Theoretical Physics, University of Geneva, 1211 Geneva, Switzerland*
[3]*Landau Institute for Theoretical Physics, 119334 Moscow, Russia*
[4]*Institut für Theorie der Kondensierten Materie, Karlsruhe Institute of Technology, 76128 Karlsruhe, Germany*
[5]*Petersburg Nuclear Physics Institute, 188350 St. Petersburg, Russia*

We study the localization and decay properties as well as the thermal conductance of one-dimensional plasmons. Our model contains a Luttinger-liquid part with spatially random plasmon velocity and interaction parameter as well as a nonlinearity that is cubic in density. The scaling of the decay rate of plasmons is obtained in several regimes. At sufficiently high frequencies, it describes the inelastic lifetime of localized plasmon excitations that crosses over to the clean result with lowering frequencies. For higher frequencies, we analyze implications of many-body-localization effects that lead to a suppression of the decay rate. We find that the thermal conductance depends in a nontrivial fashion on the system size L. Specifically, it scales as $L^{-1/2}$ for sufficiently short wires and crosses over to $L^{-2/3}$ scaling for longer wires.

I. INTRODUCTION

One-dimensional (1D) quantum systems show plenty of fascinating phenomena [1]. Interaction effects are often strong in 1D, so that the proper elementary excitations of the systems are plasmons (collective density fluctuations) and not the genuine constituent particles (fermions or bosons). The resulting state of matter is referred to as the Luttinger liquid (LL). Due to advances in technological fabrication processes, many physical realizations of quantum interacting 1D systems are experimentally available.

A research direction that has attracted a considerable amount of interest in recent years is the thermal transport and energy relaxation in various 1D setups, including systems of photons [2] and of cold atoms [3,4] as well as quantum Hall edges with counterpropagating modes [5–13]. The quantum Hall structures provide a particularly suitable experimental platform for the exploration of this class of phenomena. Recent realizations of synthetic quantum Hall edges [14,15] allow for unprecedented control of the system parameters.

Another prominent example of quantum 1D systems is the Josephson junction (JJ) chains. They were studied extensively during the last two decades in the context of the superconductor-insulator transition [16–19] and as a platform for quantum computations [20–23] and metrology [24]. The relaxation of plasmonic waves in JJ chains was probed recently via spectroscopic measurements [25], which has triggered intensive theoretical studies [26–28] of the mechanisms responsible for the broadening of bosonic states in these systems in various parameter regimes.

Disorder is inevitable in physical systems and is particularly important in low dimensions. It induces the phenomenon of Anderson localization [29] that can have a dramatic impact on transport properties. An interplay of disorder and interaction is in general a difficult problem, with various facets. In

particular, the interaction-induced inelastic processes tend to establish decoherence of excitations, thus reducing the effect of Anderson localization that is crucially based on quantum coherence. It has been realized, however, that this delocalizing effect of interaction may be suppressed (strongly or even completely) due to quantum localization in the many-body space. This has has opened a new research area of many-body localization (MBL) [30,31], see Refs. [32–34] for recent reviews. The MBL implies nonergodicity, i.e., the complete breakdown of the conventional statistical mechanics.

The precise nature of disorder and its physical consequences may vary. In a generic 1D conductor, impurities cause backscattering of charge carriers. Their interplay with interactions is highly nontrivial [35,36]. On the one hand, interactions strongly renormalize disorder seen by low-energy electrons. On the other hand, the real (as opposed to virtual) scattering processes enabled by the interactions pave the way to energy relaxation and dephasing. The interaction-induced dephasing then cuts off the singular Anderson localization corrections and is responsible for the finite electric conductivity of the system at not too strong disorder and moderate temperatures.

In the context of the JJ chain, the disorder that is commonly considered are the random stray charges. Their relevance to the properties of the system stems from the fact that they can couple directly (via the Aharonov-Casher effect) to the quantum phase slips (QPS) [37,38] that are the driving force of the quantum superconductor-insulator transition.

A disorder of a different kind can also be present and, under special circumstances, play the major role in the aforementioned systems. Specifically, if the impurity potential experienced by the electrons in a quantum wire is smooth on the scale of the Fermi wavelength, the associated backscattering is strongly suppressed and can be ignored in a wide range of parameters. On the other hand, the induced inhomogeneities

of the average electronic density cause the spatial variations of effective interaction between particles. Those variations translate then into the inhomogeneities of the Luttinger parameter entering the LL description of the system and lead to backscattering (and, as a result, to localization) of *plasmons* [39,40]. While the low-frequency charge transport is unaffected by the plasmon backscattering, the latter has a profound impact on the energy propagation in the system [41,42] causing in particular strong violation of the celebrated Wiedemann-Franz law.

In a similar manner, in JJ chains with sufficiently strong Josephson couplings, the QPS are strongly (exponentially) suppressed. The system is then superconducting from the point of view of the charge transport (at least up to exponentially low temperatures and exponentially large lengths [43] that are often beyond the practical reach). Yet, the local fluctuations of the parameters of the system (Josephson and charging energies) create disorder for plasmonic waves and alter their dynamics.

Beyond the harmonic approximation, the plasmons in the aforementioned physical setups typically interact via a local cubic interaction. For example, in quantum wires, such an interaction originates from the quadratic curvature of the dispersion relation of the genuine electrons [41,44,45]. In the clean case, the effects of the plasmonic interactions on the dynamical correlation functions were intensively discussed in recent years, leading to the emergence of the concept of nonlinear Luttinger liquids [46]. In particular, it was shown recently [47] that the cubic interaction of plasmons governs the thermal conductance of a clean LL at lowest temperatures. The resulting thermal conductance displays a nontrivial scaling with the size of the system $G(L) \propto L^{-2/3}$, the behavior also known [48,49] to occur in classical translationally invariant nonlinear 1D systems.

In this paper we investigate a LL with a spatially random Luttinger parameter and plasmon velocity as well as with a cubic interaction of bosons. Our work is largely motivated by experimental developments and prospects discussed above. The model that we consider is expected to be relevant to various realizations of correlated 1D systems. We explore the interaction-induced decay of the plasmons in its dependence on the frequency and temperature. We find that at lowest frequencies the disorder plays a minor role, and the corresponding decay rate coincides with the one found [50] previously in a clean LL, $1/\tau \propto \omega^{3/2}$. At higher frequencies, the disorder effects become crucially important. The relaxation rate grows linearly with frequency and eventually saturates due to a weak form of MBL effects. Furthermore, joint effect of disorder and plasmonic anharmonicity manifests itself in the behavior of the thermal conductance as a function of the system length L. In a short system the thermal conductance is fully controlled by disorder, yielding $G \propto L^{-1/2}$. Upon increase of L, the system crosses over to the regime where G is governed by an interplay of disorder and interaction $G \propto L^{-2/3}$.

The paper is organized as follows. In Sec. II we give a precise definition of our model. A brief discussion of the localization of the noninteracting plasmons is presented in Sec. III. In Sec. IV we investigate the interaction-induced lifetimes of plasmons in various regimes. Section V is devoted to the analysis of the thermal conductance. Finally, Sec. VI contains

a summary of our results and a discussion of prospective research directions.

II. MODEL

The Hamiltonian of our model describing plasmons in a disordered one-dimensional system consists of two parts,

$$\mathcal{H} = \mathcal{H}_0 + \mathcal{H}_1. \tag{1}$$

The quadratic part

$$\mathcal{H}_0 = \frac{1}{2\pi} \int dx \left[v(x)K(x)(\partial_x \theta)^2 + \frac{v(x)}{K(x)}(\partial_x \phi)^2 \right] \tag{2}$$

is a generic Luttinger-liquid Hamiltonian with space-dependent plasmon velocity $v(x) = v_0 + \delta v(x)$ and Luttinger parameter $K(x) = K_0 + \delta K(x)$. The random fluctuations $\delta v(x)$ and $\delta K(x)$ are assumed to have zero mean and Gaussian statistics with

$$\overline{\delta K(x)\delta K(x')} = D_K \delta(x - x'),$$
$$\overline{\delta v(x)\delta v(x')} = D_v \delta(x - x'),$$
$$\overline{\delta v(x)\delta K(x')} = D_{vK} \delta(x - x'). \tag{3}$$

The fields $\partial_x \phi$ and $\partial_x \theta$ are related to the particle density and current, respectively,

$$\partial_x \phi = -\pi \rho, \quad vK\partial_x \theta = \pi j. \tag{4}$$

They satisfy the commutation relations

$$[\phi(x), \partial_{x'}\theta(x')] = i\pi \delta(x - x'). \tag{5}$$

One particular instance of such a model is a quantum wire with smooth (on the scale of the Fermi wavelength) disorder considered in Refs. [39–41], see also Appendix A. Here the smoothness of the disorder suppresses backscattering of electrons, whereas the spatial variations of the equilibrium fermionic density translate into fluctuations of the velocity v and the effective interaction K. The parameters of our model can in this case be expressed in terms of the amplitude U_0 and the correlation length l_U of the disorder potential, see Appendix A. In particular, under the assumption of a moderate strength of the electron-electron interaction ($K_0 \sim 1$), we get

$$D_K \sim \frac{U_0^2}{\epsilon_F^2} l_U, \tag{6}$$

where ϵ_F stands for the Fermi energy.

Another physical realization of the Hamiltonian (2) is the low-energy limit of a JJ chain with sufficiently strong Josephson couplings precluding quantum phase slips [37,38]. In this case, the variances D_K, D_v, and D_{Kv} can be expressed in terms of the disorder in local Josephson and charging energies.

The interaction effects are described in our model by the cubic coupling of bosons

$$\mathcal{H}_1 = -\frac{1}{6\pi m} \int dx [3(\partial_x \theta)^2 \partial_x \phi + (\partial_x \phi)^3]. \tag{7}$$

The origin of this interaction term is particularly transparent in the case of a quantum wire. Equation (7) expresses in the bosonization language the quadratic correction $\delta\epsilon(k) = k^2/2m$ to the spectrum of the constituent fermions near the Fermi points [44,45]. It can be traced back to the dependence

of the ground state energy density of fermions with mass m [51] on the particle density and macroscopic velocity V, $E(\rho, V) = \pi^2 \rho^3/6m + m\rho V^2/2$.

If the Hamiltonian (1) is viewed as an effective low-energy field theory of a JJ chain, the anharmonicity (7) is also natural. Indeed, any perturbation allowed by symmetry is expected to appear in such an effective description, and the two terms in the square brackets in Eq. (7) are precisely the two possible perturbations of the lowest scaling dimension that can be added to the fixed-point LL Hamiltonian. Unlike the case of fermions with quadratic spectrum where the Galilean invariance enforces the equality of the coefficients in front of the aforementioned terms, no such connection exists generically in the context of JJ chains. This distinction in the description of the two systems is, however, irrelevant for us as it can only alter numerical coefficients in our results. As to the microscopic value of the "mass" m (or, more generally, of the two allowed coupling constants) in the case of JJ chains, it can be related to the ground state energy of the system, cf. discussion after Eq. (7) as well as Refs. [52,53] where a similar problem was discussed in the context of the XXZ spin model. The cubic anharmonicity (7) is thus expected to be a perturbation generically present in systems described by LL theory. In this work we treat the mass m as a model parameter, leaving aside the question of its microscopic description.

Let us emphasize that, throughout this work, we limit our consideration to the case of weak uncorrelated disorder. The strong-disorder effects (e.g., the situation of a heavy-tailed distribution of the Josephson couplings in a JJ chain [54]) or the effects of correlated disorder (arising, e.g., in the description of plasmonic modes existing on top of a pinned charge-density wave [28,55,56]) may alter significantly [54–57] the density of states and the properties of wave functions of low-energy plasmons. Their interplay with the anharmonicities in the system constitute an interesting direction for future research but is beyond the scope of the present work.

III. LOCALIZATION LENGTH OF NONINTERACTING PLASMONS

In the absence of the anharmonic term (7), the plasmons are noninteracting and get localized due to the disorder, with the localization length equal to the mean free path with respect to backward scattering. In order to evaluate the latter, we decompose the Hamiltonian into the homogeneous and disorder parts $\mathcal{H}_0 = \mathcal{H}_0^{LL} + \mathcal{H}_0^{dis}$, given by

$$\mathcal{H}_0^{LL} = \frac{1}{2\pi} \int dx \left[v_0 K_0 (\partial_x \theta)^2 + \frac{v_0}{K_0} (\partial_x \phi)^2 \right] \quad (8)$$

and

$$\mathcal{H}_0^{dis} = \frac{1}{2\pi} \int dx \, \delta v(x) \left[K_0 (\partial_x \theta)^2 + \frac{1}{K_0} (\partial_x \phi)^2 \right]$$
$$+ \frac{v_0}{2\pi} \int dx \, \delta K(x) \left[(\partial_x \theta)^2 - \frac{1}{K_0^2} (\partial_x \phi)^2 \right]. \quad (9)$$

We then compute the transport scattering rate for plasmons, treating the disorder perturbatively.

To this end, we expand the plasmonic fields ϕ and θ into normal modes according to [1]

$$\phi(x) = -\frac{i\pi}{L} \sum_{q \neq 0} \left(\frac{K_0 L|q|}{2\pi} \right)^{1/2} \frac{1}{q} e^{-iqx} (b_q^\dagger + b_{-q}),$$

$$\theta(x) = \frac{i\pi}{L} \sum_{q \neq 0} \left(\frac{L|q|}{2\pi K_0} \right)^{1/2} \frac{1}{|q|} e^{-iqx} (b_q^\dagger - b_{-q}), \quad (10)$$

where L is the system size and $b_q^{(\dagger)}$ are standard annihilation (creation) operators of bosonic states with momentum q. The homogeneous part of the Hamiltonian (2) takes the diagonal form

$$\mathcal{H}_0^{LL} = \sum_q v_0 |q| b_q^\dagger b_q + \text{const}. \quad (11)$$

The rate of scattering induced by the random fluctuations $\delta v(x)$ and $\delta K(x)$ can be extracted from the collision integral

$$I[f] = -\sum_{q'} W_{qq'}[f(q) - f(q')], \quad (12)$$

with the transition probability given by the golden rule

$$W_{qq'} = 2\pi \overline{|\langle 0|b_{q'} \mathcal{H}_0^{dis} b_q^\dagger |0\rangle|^2} \, \delta(v_0|q| - v_0|q'|). \quad (13)$$

Here $|0\rangle$ is the plasmonic vacuum, $f(q)$ is the plasmonic distribution function, and $\mathcal{H}_0^{dis}$ is the random part of the Hamiltonian, Eq. (9). The overline denotes the average with respect to the random fluctuations of $K(x)$ and $v(x)$ according to Eq. (3).

After the disorder averaging, the modulus square of the matrix element takes the form

$$\overline{|\langle 0|b_{q'} \mathcal{H}_0^{dis} b_q^\dagger |0\rangle|^2} = \frac{1}{4L} |qq'| \left\{ D_v [1 + \text{sgn}(qq')]^2 \right.$$
$$\left. + \frac{v_0^2}{K_0^2} D_K [1 - \text{sgn}(qq')]^2 \right\}. \quad (14)$$

Note that the correlations between $v(x)$ and $K(x)$ do not contribute. Moreover, the fluctuations of the velocity contribute only to forward scattering and, due to the structure of the collision integral (12), drop out of the kinetic equation. As a result, the kinetic equation describing the evolution of the distribution function of the plasmons in the presence of disorder in the parameters of the quadratic Hamiltonian $\mathcal{H}_0$ is given by

$$\frac{\partial f(q)}{\partial t} = -\frac{v_0 D_K}{K_0^2} q^2 [f(q) - f(-q)]. \quad (15)$$

From this equation we extract the elastic scattering time $\tau_{el}(\omega)$ which leads to the localization length (mean free path) of the plasmons,

$$\xi(\omega) = \frac{v_0^2 K_0^2}{2 D_K \omega^2}. \quad (16)$$

The result (16) agrees with the one obtained previously in Refs. [39–41] for a less general [58] model of disordered Luttinger liquid.

Before closing this section, let us stress that, as follows from Eq. (16), these are spatial variations of the Luttinger

parameter $K(x)$ that are responsible for the localization of plasmons that is crucial for the physics explored in this work. This makes our model drastically different from the "random conformal symmetry" models (see, e.g., Ref. [59] and references therein) that have received much attention recently. In the present language, those models are characterized by disorder in $v(x)$ alone and thus lack the localization of plasmons.

IV. DECAY OF PLASMONIC STATES

In this section we explore the impact of the nonlinear term (7) that gives rise to finite lifetime of the localized plasmonic states discussed in Sec. III. We treat the anharmonicity perturbatively, which is justified if the temperature and the considered plasmonic energies are much smaller than the (effective) Fermi energy $\omega, T \ll m v_0^2$.

Throughout this section we assume that the disorder is weak from the point of view of plasmons involved in the scattering processes: the localization length of each plasmonic state is much longer than the corresponding de Broglie wavelength v_0/ω. Comparing the de Broglie wavelength with the localization length (16), we find that this weak-disorder condition holds for all the plasmons with frequency below the threshold

$$\omega_* \equiv \frac{v_0 K_0^2}{D_K}. \tag{17}$$

Correspondingly, at low temperatures

$$T < \omega_* \tag{18}$$

the disorder is weak for all the plasmons relevant to the transport phenomena (i.e., those with the energy smaller than temperature).

The structure of this section is as follows. In Sec. IV A we compute the decay rate of localized plasmons perturbatively by using the Fermi golden rule. We then analyze the limits of applicability of this golden-rule calculation and show that it is applicable within a (generically) broad range of frequencies [determined by Eqs. (29) and (30)] but fails both at sufficiently low and sufficiently high frequencies. The inelastic scattering of plasmons in those two regimes is discussed in Secs. IV B and IV C, respectively. In Sec. IV D we summarize the results of this section, focusing on the subthermal plasmons relevant for the energy transport, and analyze the mechanism of the motion of these plasmons through the system.

A. Golden-rule analysis

In a clean Luttinger liquid, the perturbation theory in the cubic interaction of bosons is highly singular. If the linear bosonic spectrum is assumed, the cubic nonlinearity induces the one-into-two bosonic decay processes of the type shown in Fig. 1. Within the Fermi golden-rule approximation, the corresponding rate diverges due to the equivalence of the energy and momentum conservation. On the other hand, an arbitrarily small bending of the plasmonic spectrum makes it impossible to satisfy simultaneously the energy and momentum conservation in the one-into-two decay within the perturbative calculation [60]. This singularity of the golden-rule analysis
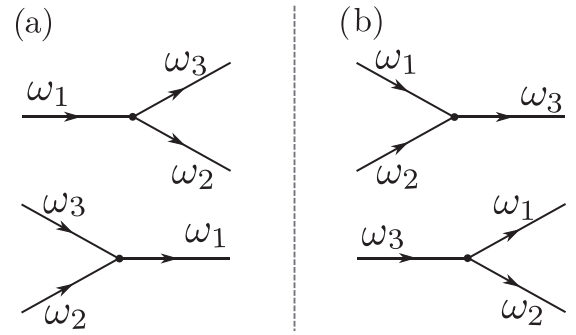

FIG. 1. Inelastic relaxation of a plasmonic mode at frequency ω_1 via (a) decay into two plasmons; (b) collision with another plasmon.

in a clean system requires a more sophisticated self-consistent analysis. We will return to this issue in Sec. IV B.

In our system, the presence of disorder breaks the momentum conservation, which makes the lowest-order golden-rule calculation well defined (i.e., not singular). Such a calculation was earlier performed in Ref. [41] where the condition $\omega \gg T$ (opposite to the regime of our main interest in this work) was implicitly assumed. We proceed now by performing the golden-rule calculation of the decay rate of localized plasmons in various ranges of frequency. After this, we will analyze the actual applicability of the golden-rule results.

We start from noninteracting plasmonic modes localized by disorder with the localization length given by Eq. (16). The quadratic Hamiltonian (2) can be diagonalized by a linear transformation of bosonic fields

$$\phi(x) = \sum_\mu \sqrt{\frac{\pi v(x) K(x)}{2\Omega_\mu}} [\psi_\mu(x) b_\mu + \psi_\mu^*(x) b_\mu^\dagger],$$

$$\partial_x \theta(x) = \frac{1}{i} \sum_\mu \sqrt{\frac{\pi \Omega_\mu}{2v(x) K(x)}} [\psi_\mu(x) b_\mu - \psi_\mu^*(x) b_\mu^\dagger], \tag{19}$$

where $\psi_\mu(x)$ are the eigenfunctions of the operator $\mathcal{D}$ defined by

$$\mathcal{D}\psi_\mu = -\sqrt{v(x)K(x)} \partial_x \left[\frac{v(x)}{K(x)} \partial_x (\sqrt{v(x)K(x)} \psi_\mu(x)) \right]$$

$$= \Omega_\mu^2 \psi_\mu, \tag{20}$$

and b_μ, $b_\mu^\dagger$ are usual bosonic operators. In this basis, the quadratic Hamiltonian takes the form

$$\mathcal{H}_0 = \sum_\mu \Omega_\mu \left[b_\mu^\dagger b_\mu + \frac{1}{2} \right]. \tag{21}$$

The eigenfrequencies of plasmonic states Ω_μ are random and possess Debye (constant in 1D) density of states at low energy (cf. discussion at the end of Sec. II).

Under the assumption of weak disorder $|q|\xi \gg 1$, we model the wave functions $\psi_\mu(x)$ by

$$\psi_\mu(x) = \frac{1}{\sqrt{\xi(\omega)}} e^{-|x-x_0|/\xi(\omega)} e^{iqx}, \quad \omega = v_0|q|, \tag{22}$$

i.e., as plane waves modulated by an exponential factor reflecting the disorder-induced localization. The index μ in

Eq. (22) comprises two parameters: the energy ω and the center of the localized state x_0. While the precise form of wave functions in a disordered 1D media varies from one eigenstates to another, their general features are well understood. Specifically, the eigenstates can be viewed as plane waves modulated by envelopes with a characteristic scale given by the localization length ξ. It is important that ξ is the only characteristic scale for the envelopes of localized states: it determines both the exponential decay rate and the extension of the core part of the wave function [61]. Thus, the ansatz (22) captures the most important features of the localized wave functions: oscillation on short length scales with a wave vector q modulated by an envelope function characterized by a single scale ξ and exponentially decaying at distances larger than ξ. In particular, Eq. (22) captures correctly the uncertainty in momentum of the plasmon and the associated broadening of the δ function expressing the momentum conservation in the scattering process. This is sufficient for our analysis in which we ignore numerical prefactors of order unity.

The inelastic scattering processes contributing to the relaxation of a bosonic mode at frequency ω_1 are shown in Fig. 1. At temperatures satisfying the inequality (18) (regardless of the relation between ω_1 and T) the processes shown in Fig. 1(b) contribute at most the same order of magnitude as the one-into-two plasmon decay shown in Fig. 1(a) (see Appendix C for details). We thus concentrate on the latter. The kinetic equation associated with the scattering processes depicted in Fig. 1(a) is given by [62]

$$\frac{\partial f(\mu_1)}{\partial t} = -\int \frac{dx_2}{L}\frac{dx_3}{L}\sum_{q_2,q_3} W_{\mu_1}^{\mu_2,\mu_3}\{f(\mu_1)[1+f(\mu_2)]$$
$$\times [1+f(\mu_3)] - [1+f(\mu_1)]f(\mu_2)f(\mu_3)\}, \quad (23)$$

where L is the system size, and $f(\mu_i)$ denotes the plasmon distribution function. Here $\mu_i \equiv [x_i, \omega(q_i)]$ characterizes a plasmon centered in the real and momentum space around x_i and q_i, respectively. The transition probability for the process reads

$$W_{\mu_1}^{\mu_2,\mu_3} = 2\pi \left|M_{\mu_1}^{\mu_2,\mu_3}\right|^2 \delta(\omega_1 - \omega_2 - \omega_3) \quad (24)$$

with the matrix element

$$M_{\mu_1}^{\mu_2,\mu_3} = \langle 0|b_{\mu_3} b_{\mu_2} \mathcal{H}_1 b_{\mu_1}^\dagger|0\rangle. \quad (25)$$

In order to extract the decay rate, we linearize the kinetic equation (23) with respect to the equilibrium state by introducing the deviation from the equilibrium (Bose) distribution, $\delta f(\mu_i) = f(\mu_i) - n_B(\omega_i)$. Within the relaxation-time approximation, the decay rate $1/\tau$ is then extracted from the diagonal part of the linearized collision integral [$\propto \delta f(\mu_1)$]. It is given by

$$\frac{1}{\tau} = \int \frac{dx_2}{L}\int \frac{dx_3}{L}\sum_{q_2,q_3} W_{(x_1,\omega_1)}^{(x_2,\omega_2),(x_3,\omega_3)}$$
$$\times [1 + n_B(\omega_2) + n_B(\omega_3)]. \quad (26)$$

Employing now Eq. (22) and estimating the resulting integrals (see Appendix B for details), we find that the

high-energy plasmons with $\omega > T$ relax at the rate

$$\frac{1}{\tau(\omega)} \sim \frac{\left(3 + K_0^2\right)^2 \xi(\omega)}{K_0 m^2 v_0^5}\omega^4, \quad \omega > T. \quad (27)$$

Here and subsequently the symbol "$\sim$" stands for the equality up to a factor of order unity (evaluation of which requires using exact statistics of wave functions of the localized plasmons). The result (27) agrees with the one found previously in Ref. [41] [see Eq. (12) of that work].

Within the linear-response regime, the thermal transport is controlled by subthermal plasmons $\omega < T$. In this regime we find the golden-rule decay rate (see Appendix B)

$$\frac{1}{\tau(\omega)} \sim \frac{\left(3 + K_0^2\right)^2 \xi(\omega)}{K_0 m^2 v_0^5}\omega^3 T, \quad \omega < T. \quad (28)$$

Equation (28) will be used below in the analysis of the thermal conductance.

We turn now to the discussion of the applicability conditions of the golden-rule calculation. The picture of localized plasmonic states decaying due to anharmonicities is only valid if the elastic scattering time $\tau_{el}(\omega) \equiv \xi(\omega)/v_0$ is shorter than the inelastic time (28). The comparison of Eqs. (16) and (28) (we focus here on the subthermal plasmons relevant for transport) reveals that this only holds for not too low frequencies,

$$\omega > \tilde{\omega} \equiv \frac{K_0^3\left(3 + K_0^2\right)^2 T}{m^2 v_0^2 D_K^2}. \quad (29)$$

For plasmons with lower frequencies $\omega < \tilde{\omega}$, the inelastic time is shorter than the elastic one. In view of this, the disorder can be ignored (in the leading approximation) when one evaluates the rate of inelastic collisions for such low frequencies. We will analyze the inelastic relaxation of plasmons in this regime in Sec. IV B.

Remarkably, the naive golden-rule approach fails not only at low ω but also at high enough frequencies. Specifically, the golden-rule treatment is justified provided that the obtained rate is larger than the level spacing of final states into which a plasmon decays, see the related discussion in the context of MBL in quantum dots [63,64] and in strongly disordered 1D electronic conductors [30,31]. In particular, for the decay processes of Fig. 1, the final states are the two-particle states (they are characterized by two frequencies ω_2 and ω_3 specifying the plasmonic modes that change their occupation as a result of the relaxation of the mode ω_1). The golden rule approach breaks down at high frequencies because the localization of plasmons becomes stronger there and the two-particle level spacing grows with frequency. In Sec. IV C we will compute the associated level spacing and show that the result (28) remains valid for

$$\omega < \bar{\omega} \equiv \left(\frac{K_0^7\left(3 + K_0^2\right)^2 T}{D_K^4 m^2}\right)^{1/3}. \quad (30)$$

The plasmons with higher energies cannot decay via the interaction with plasmons of similar energy and are in this sense in a "quasi-MBL" regime. The true MBL is, however, absent because of the possibility to relax via the interaction

with the "bath" of low-energy plasmons with frequencies $\omega < \bar{\omega}$, see Sec. IV C.

B. Low frequencies: From disordered to clean regime

As discussed in Sec. IV A, our perturbative treatment of the decay rate essentially relies on the broadening of plasmonic energy levels by disorder and breaks down at low frequencies $\omega < \tilde{\omega}$. In this low-frequency regime, the localization length is longer than the inelastic mean free path, so that disorder is essentially of no importance for the inelastic collision rate.

We have also mentioned previously that the perturbative treatment of the plasmonic decay in a clean LL is singular. The problem can be circumvented by a *self-consistent* treatment of the one-into-two decay channel [50]. The result of Ref. [50] translated to our notations reads [65]

$$\frac{1}{\tau(\omega)} \sim \frac{\left(3 + K_0^2\right) T^{1/2} \omega^{3/2}}{\sqrt{K_0} m v_0^2}. \tag{31}$$

It matches smoothly the rate (28) at $\omega = \tilde{\omega}$. Combining the both rates (28) and (31), we find

$$\frac{1}{\tau(\omega)} \sim \begin{cases} \frac{(3+K_0^2) T^{1/2} \omega^{3/2}}{\sqrt{K_0} m v_0^2}, & \omega \ll \min(T, \tilde{\omega}), \\ \frac{K_0 (3+K_0^2)^2 T \omega}{D_K m^2 v_0^3}, & \tilde{\omega} \ll \omega \ll T. \end{cases} \tag{32}$$

In Eq. (32) we implicitly assume that ω satisfies the inequality (30) such that the quasi-MBL effects discussed at the end of Sec. IV A (and in more detail in Sec. IV C below) do not matter. Note also that for very weak disorder the frequency $\tilde{\omega}$, Eq. (29), becomes larger than the temperature, so that the clean result, Eq. (31), holds for all plasmons with $\omega \lesssim T$.

It is worth noting that both lines of the result (32) can be obtained from a single self-consistent calculation. Specifically, let us introduce self-consistency in Eq. (28) by replacing $\xi(\omega)$ (that essentially represents the disorder broadening of the plasmonic levels) by $(1/\xi + 1/v_0\tau)^{-1}$. Solving the emerging equation for $1/\tau$, one recovers Eq. (32).

C. "High" frequencies: Quasi-MBL regime

The golden rule used in Sec. IV A is only applicable if the two-particle level spacing is smaller than the decay rate. In this section we estimate the single-particle as well as the two-particle level spacing (cf. a related calculation in Supplemental Material of Ref. [66]). This allows us to establish the inequality (30) marking the onset of the quasi-MBL regime where the relaxation of high-energy plasmons (those with $\omega > \bar{\omega}$) is governed by the interaction with a bath of low-energy excitations with $\omega < \bar{\omega}$. We then analyze the inelastic decay of those high-energy plasmons.

The number of plasmon modes per unit energy interval that have a finite overlap with a localized mode with energy ω at position x_1 is given by

$$N_1(\omega) \sim \int dx_2 \int \frac{dq_2}{2\pi} e^{-|x_1-x_2|/\xi(\omega_2)} \delta(\omega - v_0|q_2|) \tag{33}$$

$$= \frac{\xi(\omega)}{\pi v_0}. \tag{34}$$

The single-particle level spacing in the localization volume is thus given by

$$\Delta_1(\omega) \sim \frac{1}{N_1(\omega)} \sim \frac{v_0}{\xi(\omega)}, \tag{35}$$

in agreement with the flat density of plasmonic modes.

For the two-particle level spacing, we consider the number of different plasmon pairs that can emerge in a one-into-two decay of a plasmon with frequency ω:

$$N_2(\omega) \sim \int dx_2 \int dx_3 \int \frac{dq_2}{2\pi} \frac{dq_3}{2\pi} e^{-|x_1-x_2|/\xi(\omega_2)}$$

$$\times e^{-|x_1-x_3|/\xi(\omega_3)} \delta(\omega - \omega_2 - \omega_3) \tag{36}$$

$$= \int_0^\infty \frac{d\omega_2}{\pi v_0} \int_0^\infty \frac{d\omega_3}{\pi v_0} \xi(\omega_2) \xi(\omega_3) \delta(\omega - \omega_2 - \omega_3). \tag{37}$$

The energy integrations should be cut on the lower limit at the single-particle level spacing Δ_1 in order to cure the formal divergence. Evaluating the integral over ω_3 with the help of the δ function and using Eq. (16), we obtain

$$N_2(\omega) \sim \int_{\Delta_1(\omega)}^{\omega - \Delta_1(\omega)} d\omega_2 \frac{\omega_*^2}{(2\pi)^2} \frac{1}{\omega_2^2 (\omega - \omega_2)^2} \tag{38}$$

$$= \frac{\omega_*^2}{2\pi^2} \int_{\Delta_1}^{\omega/2} d\omega_2 \frac{1}{\omega_2^2 (\omega - \omega_2)^2}, \tag{39}$$

where ω_* is given by Eq. (17). The integral is dominated by the lower limit, yielding

$$N_2(\omega) \sim \frac{\omega_*^2}{\omega^2 \Delta_1(\omega)} \sim \frac{\omega_*^3}{\omega^4}. \tag{40}$$

Using Eq. (40), we find the corresponding two-particle level spacing:

$$\Delta_2(\omega) \sim \frac{1}{N_2(\omega)} \sim \frac{\omega^4}{\omega_*^3} \sim \frac{D_K^3 \omega^4}{v_0^3 K_0^6}. \tag{41}$$

Comparison of Eq. (41) to the golden-rule relaxation rate in the frequency range $\tilde{\omega} \ll \omega \ll T$ where the disorder is important [second line in Eq. (32)] gives the criterion (30).

We conclude that at low enough temperatures,

$$T < T_0 \equiv \frac{K_0^{7/2} \left(3 + K_0^2\right)}{m D_K^2}, \tag{42}$$

the relaxation of all the subthermal plasmons is correctly described by Eq. (32). On the other hand, for $T > T_0$, the relaxation of high-frequency modes with $\omega > \bar{\omega}$ is different: it is governed by scattering off low-frequency excitations. It is clear however that the analysis leading to Eq. (28) (see Appendix B) can be straightforwardly adapted to the present situation. Specifically, treating the scattering processes shown in Fig. 1 in the golden-rule manner, we should restrict the possible final states to those that contain a low-energy plasmon. On the technical level this corresponds to the restriction of the integration over the momentum q_2 in Eq. (B3) by $q_2 < \bar{\omega}/v_0$. Proceeding along this direction, we find that in the frequency range

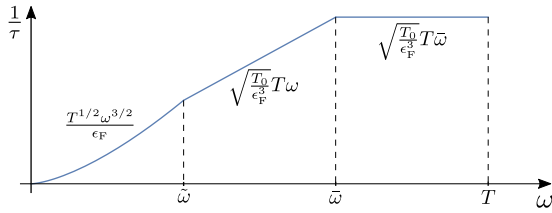$$\tilde{\omega} < \bar{\omega} < \omega < T, \tag{43}$$

FIG. 2. Schematic behavior of the inelastic scattering rate as a function of frequency, see Eqs. (32) and (44). We omit the dependence of $\tau(\omega)$ on the interaction constant K_0 (assuming interaction strength of order unity). We also assume that $T > T_0$ with temperature T_0 given by Eq. (42). The characteristic frequency scales are $\tilde{\omega} \sim T_0 T/\epsilon_F$ and $\bar{\omega} \sim (TT_0^2)^{1/3}$; they separate (from left to right) the clean, disordered, and quasi-MBL regimes.

the plasmonic decay is described by

$$\frac{1}{\tau(\omega)} \sim \frac{K_0 (3 + K_0^2)^2 T \bar{\omega}}{D_K m^2 v_0^3}, \quad \tilde{\omega} < \bar{\omega} < \omega < T. \quad (44)$$

Thus, the linear growth of the decay rate seen in the second line of Eq. (32) saturates at high frequencies due to the quasi-MBL effect. Still, the rate is finite and no genuine MBL of plasmons occurs.

D. Subthermal plasmons: Decay of plasmonic states and plasmon diffusion

In Secs. IV A, IV B, and IV C we have presented a detailed analysis of the inelastic relaxation of plasmons in a disordered LL. We now summarize the main results obtained in these sections, focusing on the subthermal plasmons. We then establish a qualitative picture of plasmon dynamics that will allow us to analyze the thermal transport in the system in Sec. V.

We assume throughout this section and in the sequel that the disorder is not too weak in the sense that the characteristic temperature T_0 defined in the inequality (42) is smaller than the high-energy scale ("Fermi energy") $\epsilon_F \equiv m v_0^2/2 \gg T$,

$$T_0 \ll \epsilon_F, \quad (45)$$

implying [see Eq. (29)] that the frequency $\tilde{\omega} < T$. In the opposite limit of very weak disorder, the latter is irrelevant for relaxation of thermal plasmons [see discussion after Eq. (32)].

Figure 2 shows the schematic behavior of the inelastic scattering rate as a function of frequency for $\omega < T$. Our results for the decay rate are expressed there in terms of the characteristic energy scales T_0, $\tilde{\omega}$, $\bar{\omega}$ [see Eqs. (42), (29), and (30)], and the high-energy scale ϵ_F. At high frequencies $\omega > \bar{\omega}$, the plasmons are in the quasi-MBL regime. Interaction with low-energy plasmons is necessary for relaxation and the relaxation rate does not depend on frequency, see Eq. (44). The quasi-MBL regime is pushed above temperature ($\bar{\omega} > T$) at low enough temperatures, $T < T_0$.

At lower frequencies $\omega < \bar{\omega}$ (or, if $T < T_0$, for all subthermal bosons), the relaxation rate is given by Eq. (32). Here two regimes can be distinguished. At intermediate frequencies $\tilde{\omega} < \omega < \bar{\omega}$ the relaxation of plasmons is appropriately described in terms of the decay of localized plasmonic modes. At lowest frequencies $\omega < \tilde{\omega}$ one can neglect the disorder in the calculation of the inelastic lifetime, viewing these plasmons

just as plane waves. [We will have, however, to recall about the presence of disorder when analyzing the contribution of these plasmons to thermal transport; see the discussion around Eq. (47).]

In Sec. V we will analyze the thermal conductance in its dependence on the system size. For that purpose it is useful to discuss first the mechanism of the bosonic transport.

At frequencies larger than $\tilde{\omega}$, disorder leads to localization of plasmons if the anharmonicity $\mathcal{H}_1$ is neglected. The relaxation induced by $\mathcal{H}_1$ goes via decay of a plasmon into two plasmons of similar energy (or recombination of two such plasmons). Typically, new plasmons are located a distance $\sim \xi(\omega)$, Eq. (16), apart from the location of the original plasmons, and the characteristic time for such a decay process is $\tau(\omega)$ as given by Eqs. (32) and (44). We can thus (somewhat loosely) think about the plasmon motion as hops between the localized states and characterize this dynamics by a (frequency-dependent) effective "diffusion coefficient" $D_{\text{eff}}(\omega)$ estimated as

$$D_{\text{eff}}(\omega) \sim \frac{\xi^2(\omega)}{\tau(\omega)} \sim \begin{cases} \dfrac{v_0^2 T_0^{3/2} T}{\epsilon_F^{1/2} \omega^3}, & \tilde{\omega} < \omega < \bar{\omega}, \\[2ex] \dfrac{v_0^2 T_0^{3/2} \bar{\omega} T}{\epsilon_F^{1/2} \omega^4}, & \bar{\omega} < \omega < T. \end{cases} \quad (46)$$

In Eq. (46) and in the sequel, we omit the dependence on the interaction constant K_0 (assuming interaction strength of order unity). It is worth noting that the energy of plasmons with given frequency is not a conserved quantity, so that $D_{\text{eff}}(\omega)$ is not a diffusion coefficient in a strict sense. Rather, it is an effective quantity that characterizes the dynamics of plasmons with frequency $\sim \omega$ at not too long timescales and thus their contribution to the thermal transport.

Let us now discuss the dynamics of plasmons at lowest energies $\omega < \tilde{\omega}$. Here plasmons are plane waves with velocity v_0 that experience inelastic collisions (decay or recombination) within the time $\tau(\omega)$ given by the first line in Eq. (32). The corresponding mean-free path is $l^{\text{in}}(\omega) = v_0 \tau(\omega)$. As in the case of higher frequencies, we ascribe to these low-frequency plasmons an effective diffusion coefficient $D_{\text{eff}}(\omega)$,

$$D_{\text{eff}}(\omega) \sim v_0 l^{\text{in}}(\omega) = v_0^2 \tau(\omega) \sim \frac{v_0^2 \epsilon_F}{T^{1/2} \omega^{3/2}}, \quad \omega < \tilde{\omega}. \quad (47)$$

While Eq. (47) looks pretty standard at first sight, it is not entirely trivial. Indeed, the scattering processes that we considered while calculating the inelastic time $\tau(\omega)$ conserve the total momentum and thus the energy current. They are thus not sufficient to establish the heat diffusion, since the latter requires some mechanism of momentum relaxation. In a *clean* LL the relaxation of the total plasmon momentum is established via the plasmon Umklapp scattering [47,67] that in the fermionic description of the LL corresponds to the equilibration of the number of left- and right-moving fermions. The latter is possible only via the diffusion of a deep hole in a Fermi sea through the bottom of the energy band and is thus exponentially suppressed at low temperatures. In the present case of a *disordered* LL there is a much more efficient mechanism of relaxing the bosonic momentum: the backscattering of a plasmon by randomness. The crucial role of this mechanism is obvious in Eq. (46) which describes a
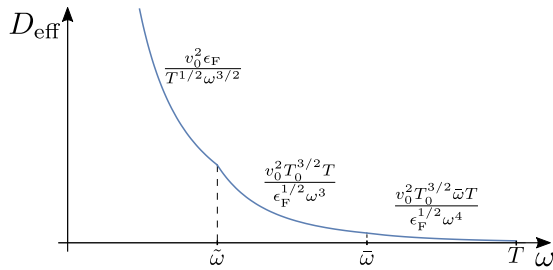
FIG. 3. Schematic behavior of the effective diffusion coefficient as predicted by Eqs. (47) and (46). We omit the dependence of $D_{\mathrm{eff}}(\omega)$ on the interaction constant K_0 (assuming interaction strength of order unity). We also assume that $T > T_0$ with temperature T_0 given by Eq. (42). The characteristic frequency scales are $\tilde{\omega} \sim T_0 T/\epsilon_{\mathrm{F}}$ and $\bar{\omega} \sim (T T_0^2)^{1/3}$.

hoppinglike relaxation of localized states. Correspondingly, the strength of the disorder enters explicitly Eq. (46) via T_0 and $\bar{\omega}$. But where is the disorder in the derivation of Eq. (47)? The answer is as follows. Considering the evolution of an initial low frequency plasmon with $\omega < \tilde{\omega}$, we make two important observation: (i) in an inelastic scattering process contributing to $\tau(\omega)$, the plasmons that are created or annihilated can typically have energies that are larger than ω by a factor ~ 2; (ii) the rate of inelastic scattering grows with frequency as $\omega^{3/2}$. It follows that the energy of the ω plasmon is transported to higher frequencies $\sim \tilde{\omega}$ within a time $\sim \tau(\omega)$. Since the disorder-induced backscattering time $\xi(\tilde{\omega})/v_0$ is equal to $\tau(\tilde{\omega})$ and thus is much shorter than $\tau(\omega)$, the overall "transport" scattering time at which the relaxation of the momentum of the ω plasmon takes place is $\sim \tau(\omega)$. This provides a justification to Eq. (47). It is worth stressing that, in this argument, we have used the condition $\tilde{\omega} < T$, which implies that the disorder is not too weak.

The behavior of the effective diffusion coefficient as predicted by Eqs. (46) and (47) is summarized in Fig. 3. In the next section we will use these results to explore the dependence of the thermal conductance of the disordered LL on the length of the system.

Before closing this section, let us discuss the feasibility of probing the relaxation of disordered plasmons experimentally. The characteristic energy scales related to the plasmon dynamics (ω_*, T_0, $\tilde{\omega}$, and $\bar{\omega}$) may vary significantly depending on the specific experimental setup and on parameters of disorder. In particular, in the case of quantum wires realized in the GaAs/AlGaAs heterostructures, details of the fabrication process (such as position of the doping layer) can alter dramatically both the magnitude and the smoothness of the disorder potential, see, e.g., Refs. [68–75] and references therein. Taking as an example heterostructure parameters discussed (in close connection to experiments) in Refs. [76,77], we observe that they were characterized by the disorder potential comparable to the Fermi energy ($\epsilon_{\mathrm{F}} \sim 5$ meV) and the disorder correlation length l_U exceeding the Fermi wavelength by a factor of ~ 5. This implies $T_0 \sim \epsilon_{\mathrm{F}}(\lambda_{\mathrm{F}}/l_U)^2 \sim 1$ K [see Eqs. (6) and (42)] and [see Eq. (17)] $\omega_* \sim T_0 l_U/\lambda_{\mathrm{F}} \sim 10$ K. Assuming now the temperature T to lie in between T_0 and ω_*, e.g., $T \sim 5$ K, one obtains the frequencies $\tilde{\omega}$ and $\bar{\omega}$ in the GHz range: $\tilde{\omega} \sim T_0 T/\epsilon_{\mathrm{F}} \sim 100$ mK ~ 2 GHz and $\bar{\omega} \sim$

$(T T_0^2)^{1/3} \sim 1.5$ K ~ 30 GHz. These values of the characteristic temperature and of the frequency scales separating different regimes (see Fig. 2) demonstrate that the plasmonic relaxation studied in this work should be experimentally accessible. Furthermore, the aforementioned flexibility of parameters of fabricated structures is favorable for tuning the characteristic scales in order to optimize experimental measurements. While we have presented explicit values only for semiconductor quantum wires, we expect that experimental studies of the plasmon relaxation should be feasible also in other realizations of interacting 1D systems discussed in Sec. I.

V. THERMAL CONDUCTANCE

We are now in a position to study the thermal transport in a disordered LL. Let us consider a system of length L connected to two reservoirs with slightly different temperatures $T_R - T_L = \Delta T$. In the linear-response regime that we are considering, the thermal current j_E is proportional to the temperature difference

$$j_E = G\Delta T, \tag{48}$$

where G is the thermal conductance. Our goal in this section is to determine the behavior of G and, in particular, its dependence on L.

The thermal current induced by the temperature gradient can be divided into two parts. First, since the scattering processes become progressively weaker with lowering frequency, plasmons with a sufficiently low energy

$$\omega < \omega_c(L) \tag{49}$$

traverse the whole system ballistically. Here $\omega_c(L)$ is the cutoff frequency for the ballistic motion that will be determined below. The energy current carried by the ballistic plasmons is given by

$$j_E^{\mathrm{bal}} = 2 \int_0^{\omega_c} \frac{d\omega}{2\pi} \omega[n_L(\omega) - n_R(\omega)], \tag{50}$$

where n_R and n_L denote the Bose distributions in the reservoirs. Using the low-frequency asymptotics of the Bose distribution $n_i(\omega) \simeq T_i/\omega$, we find that the corresponding contribution to the thermal conductance is given, up to a numerical coefficient, by the cutoff frequency:

$$G^{\mathrm{bal}}(L) = \frac{\omega_c(L)}{\pi}. \tag{51}$$

It remains to understand the cutoff for the ballistic motion. For comparatively short systems, $L < \xi(\tilde{\omega})$, the process that cuts off the ballistic propagation is the elastic scattering, so that $\omega_c(L)$ is defined by the equation

$$\xi(\omega_c) = L, \quad L < \xi(\tilde{\omega}). \tag{52}$$

On the other hand, in a longer system the ballistic contribution is cut off by the inelastic length $l^{\mathrm{in}}(\omega) = v_0 \tau(\omega)$ with τ given by the first line of Eq. (32). This length limits the ballistic motion of a low-frequency plasmon due to a combined effect of the anharmonicity and disorder, see Eq. (47) and discussion after it. We thus get the condition on $\omega_c(L)$ for long systems:

$$v_0\tau(\omega_c) = L, \quad L > \xi(\tilde{\omega}). \tag{53}$$

Employing Eqs. (16), (32), and (51), we finally obtain the contribution of ballistic plasmons to the thermal conductance:

$$G^{\text{bal}}(L) \sim \begin{cases} \frac{T_0^{1/4} \epsilon_{\text{F}}^{1/4} v_0^{1/2}}{L^{1/2}}, & L < \xi(\tilde{\omega}), \\ \frac{\epsilon_{\text{F}}^{2/3} v_0^{2/3}}{T^{1/3} L^{2/3}}, & L > \xi(\tilde{\omega}). \end{cases} \quad (54)$$

The bosons with frequency larger than $\omega_c(L)$ provide the second contribution to the thermal transport. As they travel diffusively, their contribution is characterized by a thermal *conductivity* κ that can be related to the effective diffusion coefficient $D_{\text{eff}}(\omega)$, Eqs. (46) and (47),

$$\kappa(L) \simeq T \int_{\omega_c(L)}^{T} d\omega \, D_{\text{eff}}(\omega). \quad (55)$$

The corresponding contribution to the thermal conductance of the sample is

$$\delta G(L) = \frac{\kappa(L)}{L}. \quad (56)$$

It is now easy to verify that the integration in Eq. (55) is dominated by the lower limit and reproduces the ballistic contribution (54). The full thermal conductance $G(L) = G^{\text{bal}}(L) + \delta G(L)$ of the system is thus correctly described by the ballistic result, Eq. (54), governed by plasmons with frequencies $\omega \sim \omega_c(L)$ (i.e., those on the upper border of the ballistic range of frequencies). The plasmons with $\omega \gg \omega_c(L)$ contributing to δG yield in addition only subleading (in powers of $1/L$) terms.

We thus conclude that the dependence of the thermal conductance of a disordered [in the sense of $K(x)$] nonlinear LL on the size of the system is given by Eq. (54). In comparatively short samples, it is determined solely by the elastic scattering and our result reproduces the $L^{-1/2}$ scaling found previously [41,57,78] within the harmonic approximation. In longer systems, $L > \xi(\tilde{\omega})$, the anharmonicity (or, equivalently, the plasmon interaction) plays a crucial role. We find that $G(L)$ scales in this regime as $G(L) \propto L^{-2/3}$. The same scaling, known from studies of clean classical systems at high temperature [48,49], was recently predicted to occur in a clean LL [47] but only for exponentially long system sizes (larger than the plasmon Umklapp mean free path).

VI. SUMMARY AND DISCUSSION

We have studied the relaxation of plasmonic modes and thermal transport in a Luttinger liquid with spatially random velocity and interaction parameter as well as a cubic anharmonicity. Within the harmonic approximation, the disorder in K leads to localization of plasmons with the localization length $\xi \propto 1/\omega^2$, in agreement with previous findings.

The anharmonicity leads to the interaction among plasmons, which induces relaxation of plasmonic modes. Figure 2 summarizes our results for the plasmonic decay rate at low temperatures. At low frequencies, $\omega < \tilde{\omega}$, the localization length is longer than the inelastic mean free path. The resulting scaling of the relaxation rate $1/\tau \propto \omega^{3/2}$ coincides with the corresponding result for a clean LL [50]. At higher frequencies the disorder effects set in, and the rate scales linearly, $1/\tau \propto \omega$, until saturation above the frequency $\bar{\omega}$ [given by

Eq. (30)] where the plasmons enter the quasi-MBL regime. Such "high-energy" ($\omega \gg \bar{\omega}$) plasmons cannot relax via interactions with plasmons of similar frequency due to MBL-like physics. The true MBL cannot develop, however, because of the interaction with the plasmonic bath at low energies. This mechanism of the destruction of MBL bears a certain similarity to the one known [79] for continuous disordered fermionic models where the unbounded growth of the single-particle localization length at high energies paves the way for relaxation. An important difference in our case in comparison to the fermionic models is the presence of the bath at *low* energies. The relaxation assisted by such a bath does not require exponentially rare events and is thus suppressed only in a power-law fashion in comparison to the naive golden-rule result.

We have analyzed the plasmon dynamics and demonstrated that it can be characterized by an effective diffusion coefficient $D_{\text{eff}}(\omega)$ whose frequency dependence is summarized in Fig. 3. At low frequencies, $\omega < \tilde{\omega}$, where $\tilde{\omega}$ is given by Eq. (29), the fastest scattering mechanism is the inelastic scattering that transports the plasmon energy flux towards higher frequencies where it is backscattered by disorder. As a result, $D_{\text{eff}}(\omega)$ is determined by the inelastic scattering rate. At higher frequencies, $\omega > \tilde{\omega}$ the plasmon dynamics can be visualized as interaction-induced hops between localized states.

The thermal conductance $G(L)$ of the disordered LL shows a nontrivial scaling with the size of the system L, see Eq. (54). The conductance $G(L)$ is dominated by the low-frequency plasmons that are ballistic on the scale of the system size. Upon increase of the size of the system, the scaling of $G(L)$ crosses over from $G(L) \propto L^{-1/2}$ (effectively noninteracting plasmons) to $G(L) \propto L^{-2/3}$. The latter result does not contain the disorder explicitly as it derives from the inelastic scattering length in a clean system. However, the disorder enters implicitly through the condition $\tilde{\omega} \ll T$, which implies that the disorder is not too weak.

Before closing this paper, let us discuss possible extensions of our work. First, as was pointed out in Secs. II and IV, we have limited our consideration to the case of not too strong, uncorrelated disorder and weak anharmonicity. The strong-disorder effects and/or the correlated nature of disorder may alter significantly [54–57] the density of states and the localization properties of the single-particle wave functions of the low-energy plasmons. Implications of the anharmonic coupling of plasmons in such systems as well as effects of stronger plasmonic interactions constitute an interesting direction for future research.

Second, one can include in the model the fermionic backscattering (or, equivalently, QPS in the context of the JJ chains). We remind the reader that we have not included such terms in view of their exponential smallness, see Sec. I. On the other hand, the fermionic backscattering in a LL grows under the renormalization group for a repulsive interaction (or a not too strong attraction). In this situation it will modify the ultimate infrared behavior of the system.

A further ingredient that was discarded in our analysis is the curvature of the plasmonic spectrum. While it is not expected to affect the low-frequency (and thus large-L) behavior, it may influence significantly the inelastic relaxation of plasmons at intermediate frequencies, cf. Ref. [47]. In the context of JJ chains, both the curvature of plasmons and the

QPS are of direct relevance to spectroscopy of real physical systems [25].

Finally, and on a more general note, it would be interesting to explore possible connections between the model of the K-disordered nonlinear LL and problems of the generalized 1D hydrodynamics [80–87] that currently attract much attention.

APPENDIX A: RELATION TO MODEL OF FLUCTUATING ELECTRON DENSITY

In this Appendix we give a brief account of the derivation of the Hamiltonian (1) in the context of a quantum wire with smooth disorder potential [39–41] and establish the correspondence of our notations to those of Ref. [41].

We consider a quantum wire subject to an external disorder potential $U(x)$ that is smooth on the scale of the Fermi wavelength λ_F. The backscattering of electrons by the disorder requires momentum transfer of $2k_F$ and is exponentially small in this case. The disorder induces however spatial variations of the equilibrium electronic density

$$n_{eq}(x) = n_0 + \delta n_{eq}(x) \tag{A1}$$

that can alter significantly the dynamics of plasmonic excitations in the system.

The density fluctuations $\delta n_{eq}(x)$ are assumed to be small and thus Gaussian. Furthermore, we assume that, while the correlation length l_U of potential fluctuations is much longer than the Fermi wavelength ($l_U \gg \lambda_F$), it is still small compared to the wavelength of the thermal plasmons. Under these assumptions, the statistics of δn_{eq} is fully specified by the correlation function

$$\overline{\delta n_{eq}(x)\delta n_{eq}(x')} = n_0^2 l_D \delta(x - x'), \tag{A2}$$

where the parameter l_D (with dimension of length) measures the strength of the fluctuations. It can be expressed in terms of the amplitude U_0 of the potential fluctuations and the correlation length l_U,

$$l_D \sim \frac{1}{\epsilon_F^2} \int dx \langle U(x)U(0)\rangle \sim \left(\frac{U_0}{\epsilon_F}\right)^2 l_U. \tag{A3}$$

Here ϵ_F is the Fermi energy and we assume that $U_0 \lesssim \epsilon_F$.

Within the hydrodynamic approximation the dynamical state of the electronic fluid is described by the momentum density (momentum per unit volume) $p(x)$ and the displacement field $u(x)$ (displacement of fluid particles from their equilibrium positions) that is related to the (dynamical) density of the electronic fluid by

$$n(x, t) - n_{eq}(x) = -\frac{d}{dx}[n_{eq}u]. \tag{A4}$$

The momentum density p and displacement u are canonically conjugate variables and on the quantum level satisfy the commutation relation

$$[\hat{u}(x), \hat{p}(x')] = i\delta(x - x'). \tag{A5}$$

In the harmonic approximation, the Hamiltonian of the system can be written as $\mathcal{H}_0^{FHK} = \int dx H_0^{FHK}(x)$ [41] with

$$H_0^{FHK}(x) = \frac{p^2}{2mn_{eq}(x)} + \frac{1}{2}\left(V_0 + \frac{\pi^2}{m}n_{eq}(x)\right)\left(\frac{d[n_{eq}u]}{dx}\right)^2. \tag{A6}$$

The first term in Eq. (A6) represents the kinetic energy of the fluid motion while the second term gives the energy arising due to variations of the density of the fluid. It consists of two contributions. The first one is due to electron-electron interaction and (under the assumption of good screening) is proportional to the zero-momentum component of the interaction V_0. The second contribution originates from the density dependence of the ground-state energy of the noninteracting Fermi gas.

The fields p and u in Eq. (A6) are related to the fields θ and ϕ introduced in the main text by

$$\frac{1}{\pi}\phi(x) = n_{eq}(x)u(x), \quad \partial_x\theta(x) = \frac{1}{n_{eq}(x)}p(x). \tag{A7}$$

With this identification of variables one immediately sees that Eq. (A6) is a special case of our general model (2) where both $K(x)$ and $v(x)$ are expressed in terms of a single random function $n(x)$:

$$v(x) = \frac{1}{m}\sqrt{n(x)[\pi^2 n(x) + mV_0]},$$

$$K(x) = \frac{\pi\sqrt{n(x)}}{\sqrt{\pi^2 n(x) + mV_0}},$$

$$K_0 = \frac{\pi\sqrt{n_0}}{\sqrt{\pi^2 n_0 + mV_0}} = g,$$

$$D_K = \frac{K_0^2}{4}(1 - K_0^2)^2 l_D = \frac{g^6 V_0^2 l_D}{4\pi^2 v_F^2}. \tag{A8}$$

Here $v_F \equiv \pi n_0/m$ denotes the Fermi velocity. Equations (A8) provide the explicit correspondence between the notations of the present work and that of Ref. [41].

Up to now we were discussing the Hamiltonian of the system within the harmonic approximation. The anharmonic corrections originate from the curvature of the fermionic spectrum in the quantum wire near the Fermi level. To derive them, one can neglect the (small) fluctuations of the equilibrium density. The result is given by Eq. (7) of the main text (see discussion after Eq. (7) as well as Refs. [44,45]). Using the identification of the dynamical variables and the basic parameters of the models, as given by Eqs. (A7) and (A8), one can check that Eq. (7) is identical [88] to Eq. (11) of Ref. [41].

APPENDIX B: DETAILS OF THE PERTURBATIVE CALCULATION OF THE DECAY RATE

In this Appendix we present details of the golden-rule calculations of the plasmon decay rate leading to Eqs. (28) and (27).

We begin by explicitly computing the matrix element (25). Making use of the transformation (19), we express the nonlinearity (7) in terms of bosonic operators. [Here we can set $v(x) = v_0$ and $K(x) = K_0$ in Eq. (19).] The evaluation of the

vacuum expectation value in Eq. (25) yields

$$\langle 0|b_{\mu_3}b_{\mu_2}\mathcal{H}_1 b_{\mu_1}^{\dagger}|0\rangle \simeq \frac{i\sqrt{\pi}}{2\sqrt{2}m\sqrt{K_0}}\left(3+K_0^2\right)\sqrt{|q_1 q_2 q_3|}$$
$$\times \int dx\,\psi_{\mu_1}(x)\psi_{\mu_2}^*(x)\psi_{\mu_3}^*(x). \quad \text{(B1)}$$

$$\frac{1}{\tau(q_1)} = \frac{\pi^2\left(3+K_0^2\right)^2}{4v_0 K_0 m^2 L^2}\sum_{q_2,q_3}|q_1 q_2 q_3|\delta(|q_1|-|q_2|-|q_3|)[1+n_{\rm B}(\omega_2)+n_{\rm B}(\omega_3)]\int dx\,dx'\,e^{i(q_1-q_2-q_3)(x-x')}$$
$$\times \left(1+\frac{|x-x'|}{\xi_2}\right)e^{-|x-x'|/\xi_2}\left(1+\frac{|x-x'|}{\xi_3}\right)e^{-|x-x'|/\xi_3}\frac{1}{\xi_1}e^{-|x-x_1|/\xi_1}e^{-|x'-x_1|/\xi_1}, \quad \text{(B2)}$$

where $\omega_i = \omega(q_i) = v_0|q_i|$ and $\xi_i = \xi(\omega_i)$. After introducing relative $(r = x - x')$ and center-of-mass $[R = (x + x')/2]$ coordinates, we perform the integration over R and estimate the integration over r by cutting the integral at the upper limit at ξ_1. In the limit $L \to \infty$, the sums over q_2 and q_3 are replaced by the integrations and we get

$$\frac{1}{\tau(q_1)} \sim \frac{\left(3+K_0^2\right)^2}{v_0 K_0 m^2}\int dq_2\int dq_3|q_1 q_2 q_3|$$
$$\times \frac{\sin[(q_1-q_2-q_3)\xi_1]}{q_1-q_2-q_3}\delta(|q_1|-|q_2|-|q_3|)$$
$$\times [1+n_{\rm B}(\omega_2)+n_{\rm B}(\omega_3)]. \quad \text{(B3)}$$

The integration over q_3 can be performed by exploiting the delta function, the remaining integral over q_2 can be estimated in different limits. In the case of $\omega_1 = v_0|q_1| \ll T$, the Bose functions can be approximated by their low-frequency behavior $n_B(\omega) \simeq T/\omega$. Characteristic values of q_2 in the above integral are of the order of q_1. We obtain in this limit

$$\frac{1}{\tau(\omega_1)} \sim \frac{\left(3+K_0^2\right)^2\xi(\omega_1)}{K_0 m^2 v_0^5}\omega_1^3 T, \quad \omega_1 \ll T, \quad \text{(B4)}$$

which is Eq. (28) of the main text. In the opposite limit of high frequencies, $\omega_1 \gg T$, unity is a dominant term in the square brackets in Eq. (B3) and characteristic values of q_2 are of the order of q_1. We thus arrive at

$$\frac{1}{\tau(\omega_1)} \sim \frac{\left(3+K_0^2\right)^2\xi(\omega_1)}{K_0 m^2 v_0^5}\omega_1^4, \quad \omega_1 \gg T, \quad \text{(B5)}$$

which is Eq. (27) of the main text.

APPENDIX C: SCATTERING PROCESS INVOLVING A COLLISION WITH ANOTHER PLASMON

In this Appendix we study the processes depicted in Fig. 1(b), which involve a collision with another plasmon. We show here that processes of this kind contribute at most the same amount to the decay rate as the processes where the plasmon decays into two plasmons [depicted in Fig. 1(a)].

The analysis of this kind of processes goes along the lines of Sec. IV A and Appendix B. In comparison to Eq. (23), the collision integral has a slightly different structure with respect

We have assumed here that the disorder is not too strong, in the sense of the condition (18), i.e., the localization lengths of involved states are larger than the corresponding wavelengths $|q_i|\xi(\omega_i) \gg 1$. In view of this, we have the approximations $\psi_{\mu_i}'(x) \simeq iq_i\psi_{\mu_i}(x)$ as well as $\Omega_{\mu_i} \simeq \omega(q_i)$. Inserting this result for the matrix element into Eq. (26) and performing the integrations over x_2 and x_3 yields

to the distribution functions,

$$\frac{\partial f(\mu_1)}{\partial t} = -\int\frac{dx_2}{L}\frac{dx_3}{L}\sum_{q_2,q_3}\tilde{W}_{\mu_1,\mu_2}^{\mu_3}\{f(\mu_1)f(\mu_2)[1+f(\mu_3)]$$
$$-[1+f(\mu_1)][1+f(\mu_2)]f(\mu_3)\}. \quad \text{(C1)}$$

Here the transition probability for the process is given by [cf. Eq. (24)]

$$\tilde{W}_{\mu_1,\mu_2}^{\mu_3} = 2\pi\left|\tilde{M}_{\mu_1,\mu_2}^{\mu_3}\right|^2\delta(\omega_1+\omega_2-\omega_3),$$
$$\mu_i = [x_i, \omega(q_i)], \quad \text{(C2)}$$

with the matrix element [cf. Eq. (25)]

$$\tilde{M}_{\mu_1,\mu_2}^{\mu_3} = \langle 0|b_{\mu_3}\mathcal{H}_{\rm int}b_{\mu_2}^{\dagger}b_{\mu_1}^{\dagger}|0\rangle = \left(M_{\mu_3}^{\mu_2,\mu_1}\right)^*. \quad \text{(C3)}$$

Linearizing the collision integral by expanding in $\delta f(\mu_i) = f(\mu_i) - n_{\rm B}(\omega_i)$ and extracting the diagonal part yields the golden-rule-type expression for the decay rate associated with the processes depicted in Fig. 1(b),

$$\frac{1}{\tau} = \int dx_2\int dx_3\int\frac{dq_2}{2\pi}\int\frac{dq_3}{2\pi}\left|\tilde{W}_{\mu_1,\mu_2}^{\mu_3}\right|^2$$
$$\times [n_{\rm B}(\omega_2)-n_{\rm B}(\omega_3)]. \quad \text{(C4)}$$

The main differences to the expression of the decay rate corresponding to the processes depicted in Fig. 1(a), Eq. (26), are the combination of the Bose functions and the delta function associated with the energy conservation [compare Eqs. (24) and (C2)]. Inserting the expression for the transition probability (C2) and the matrix element (B1), we arrive at

$$\frac{1}{\tau(q_1)} \sim \frac{\left(3+K_0^2\right)^2}{v_0 K_0 m^2}\int dq_2\int dq_3|q_1 q_2 q_3|$$
$$\times \frac{\sin[(q_1+q_2-q_3)\xi_3]}{q_1+q_2-q_3}\delta(|q_1|+|q_2|-|q_3|)$$
$$\times [n_{\rm B}(\omega_2)-n_{\rm B}(\omega_3)], \quad \text{(C5)}$$

which is a counterpart of Eq. (B3). Note also the difference in the argument of the sine function compared to Eq (B3). Here the shortest of the three localization lengths (ξ_1, ξ_2, ξ_3) enters. In the case of the processes shown in Fig. 1(b) it is ξ_3, while for those in Fig. 1(a) it is ξ_1 [cf. the discussion before Eq. (B3)]. The integration over q_3 can be performed by exploiting the energy conservation.

Finally, the remaining integral over q_2 can be estimated in different regimes: At low temperatures $T \ll \omega_1$, the Bose function of plasmon 3 does not contribute significantly. The characteristic value in the integral is $q_2 = T/v_0$ and the Bose function of plasmon 2 can be approximated by T/ω_2. As a result, we obtain

$$\frac{1}{\tau(\omega_1)} \sim \frac{\left(3 + K_0^2\right)^2}{K_0 m^2 v_0^5} \xi(\omega_1) \omega_1^2 T^2, \quad T \ll \omega_1. \quad (C6)$$

Thus, at energies much higher than the temperature, the processes depicted in Fig. 1(b) are subleading compared to the ones in Fig. 1(a), cf. Eq. (27).

In the case of high temperatures, $\omega_1 \ll T$, the characteristic value in the integral is $q_2 = q_1$. Both Bose functions contribute and can be approximated by $n_B(\omega_i) = T/\omega_i$. We find

$$\frac{1}{\tau(\omega_1)} \sim \frac{\left(3 + K_0^2\right)^2}{K_0 m^2 v_0^5} \xi(\omega_1) \omega_1^3 T, \quad \omega_1 \ll T. \quad (C7)$$

As can be seen, in the high-temperature regime, $\omega_1 \ll T$, we find the same behavior as for the processes depicted in Fig. 1(a), Eq. (28).

[1] T. Giamarchi, *Quantum Physics in One Dimension*, International series of monographs on physics 121 (Clarendon, Oxford, 2004).

[2] M. Meschke, W. Guichard, and J. P. Pekola, Nature (London) **444**, 187 (2006).

[3] J.-P. Brantut, C. Grenier, J. Meineke, D. Stadler, S. Krinner, C. Kollath, T. Esslinger, and A. Georges, Science **342**, 713 (2013).

[4] D. Husmann, M. Lebrat, S. Häusler, J.-P. Brantut, L. Corman, and T. Esslinger, Proc. Natl. Acad. Sci. **115**, 8563 (2018).

[5] H. le Sueur, C. Altimiras, U. Gennser, A. Cavanna, D. Mailly, and F. Pierre, Phys. Rev. Lett. **105**, 056803 (2010).

[6] C. Altimiras, H. le Sueur, U. Gennser, A. Anthore, A. Cavanna, D. Mailly, and F. Pierre, Phys. Rev. Lett. **109**, 026803 (2012).

[7] V. Venkatachalam, S. Hart, L. Pfeiffer, K. West, and A. Yacoby, Nat. Phys. **8**, 676 (2012).

[8] S. Jezouin, F. D. Parmentier, A. Anthore, U. Gennser, A. Cavanna, Y. Jin, and F. Pierre, Science **342**, 601 (2013).

[9] H. Inoue, A. Grivnin, Y. Ronen, M. Heiblum, V. Umansky, and D. Mahalu, Nat. Commun. **5**, 4067 (2014).

[10] E. Sivre, A. Anthore, F. D. Parmentier, A. Cavanna, U. Gennser, A. Ouerghi, Y. Jin, and F. Pierre, Nat. Phys. **14**, 145 (2017).

[11] A. Rosenblatt, F. Lafont, I. Levkivskyi, R. Sabo, I. Gurman, D. Banitt, M. Heiblum, and V. Umansky, Nat. Commun. **8**, 2251 (2017).

[12] M. Banerjee, M. Heiblum, A. Rosenblatt, Y. Oreg, D. E. Feldman, A. Stern, and V. Umansky, Nature (London) **545**, 75 (2017).

[13] M. Banerjee, M. Heiblum, V. Umansky, D. E. Feldman, Y. Oreg, and A. Stern, Nature (London) **559**, 205 (2018).

[14] M. G. Prokudina, S. Ludwig, V. Pellegrini, L. Sorba, G. Biasiol, and V. S. Khrapai, Phys. Rev. Lett. **112**, 216402 (2014).

[15] Y. Cohen, Y. Ronen, W. Yang, D. Banitt, J. Park, M. Heiblum, A. D. Mirlin, Y. Gefen, and V. Umansky, Nat. Commun. **10**, 1920 (2019).

[16] E. Chow, P. Delsing, and D. B. Haviland, Phys. Rev. Lett. **81**, 204 (1998).

[17] D. Haviland, K. Andersson, and P. Ågren, J. Low Temp. Phys. **118**, 733 (2000).

[18] W. Kuo and C. D. Chen, Phys. Rev. Lett. **87**, 186804 (2001).

[19] K. Cedergren, R. Ackroyd, S. Kafanov, N. Vogt, A. Shnirman, and T. Duty, Phys. Rev. Lett. **119**, 167701 (2017).

[20] V. E. Manucharyan, J. Koch, L. I. Glazman, and M. H. Devoret, Science **326**, 113 (2009).

[21] J. Koch, V. Manucharyan, M. H. Devoret, and L. I. Glazman, Phys. Rev. Lett. **103**, 217004 (2009).

[22] L. B. Nguyen, Y.-H. Lin, A. Somoroff, R. Mencia, N. Grabon, and V. E. Manucharyan, arXiv:1810.11006.

[23] U. Vool, I. M. Pop, K. Sliwa, B. Abdo, C. Wang, T. Brecht, Y. Y. Gao, S. Shankar, M. Hatridge, G. Catelani, M. Mirrahimi, L. Frunzio, R. J. Schoelkopf, L. I. Glazman, and M. H. Devoret, Phys. Rev. Lett. **113**, 247001 (2014).

[24] W. Guichard and F. W. J. Hekking, Phys. Rev. B **81**, 064508 (2010).

[25] R. Kuzmin, R. Mencia, N. Grabon, N. Mehta, Y.-H. Lin, and V. E. Manucharyan, Nat. Phys. **15**, 930 (2019), see also the associated News & Views article, A.D. Mirlin and I.V. Protopopov, *ibid.* **15**, 880 (2019).

[26] M. Bard, I. V. Protopopov, and A. D. Mirlin, Phys. Rev. B **98**, 224513 (2018).

[27] H.-K. Wu and J. D. Sau, Phys. Rev. B **99**, 214509 (2019).

[28] M. Houzet and L. I. Glazman, Phys. Rev. Lett. **122**, 237701 (2019).

[29] E. Abrahams, *50 Years of Anderson Localization*, International journal of modern physics: Condensed matter physics, statistical physics, applied physics (World Scientific, Singapore, 2010).

[30] I. V. Gornyi, A. D. Mirlin, and D. G. Polyakov, Phys. Rev. Lett. **95**, 206603 (2005).

[31] D. Basko, I. Aleiner, and B. Altshuler, Ann. Phys. **321**, 1126 (2006).

[32] R. Nandkishore and D. A. Huse, Ann. Rev. Condens. Matter Phys. **6**, 15 (2015).

[33] F. Alet and N. Laflorencie, C. R. Phys. **19**, 498 (2018).

[34] D. A. Abanin, E. Altman, I. Bloch, and M. Serbyn, Rev. Mod. Phys. **91**, 021001 (2019).

[35] T. Giamarchi and H. J. Schulz, Phys. Rev. B **37**, 325 (1988).

[36] I. V. Gornyi, A. D. Mirlin, and D. G. Polyakov, Phys. Rev. B **75**, 085421 (2007).

[37] R. M. Bradley and S. Doniach, Phys. Rev. B **30**, 1138 (1984).

[38] K. A. Matveev, A. I. Larkin, and L. I. Glazman, Phys. Rev. Lett. **89**, 096802 (2002).

[39] A. Gramada and M. E. Raikh, Phys. Rev. B **55**, 7673 (1997).

[40] A. Gramada and M. E. Raikh, Phys. Rev. B **55**, 1661 (1997).

[41] R. Fazio, F. W. J. Hekking, and D. E. Khmelnitskii, Phys. Rev. Lett. **80**, 5611 (1998).

[42] M. Filippone, F. Hekking, and A. Minguzzi, Phys. Rev. A **93**, 011602(R) (2016).

[43] The QPS amplitude is exponentially small in the parameter $\sqrt{E_J/E_C}$, where E_J is the Josephson energy and E_C is the charging energy of the junction [38,89].

[44] M. Schick, Phys. Rev. **166**, 404 (1968).

[45] A. Jevicki and B. Sakita, Nucl. Phys. B **165**, 511 (1980).

[46] A. Imambekov, T. L. Schmidt, and L. I. Glazman, Rev. Mod. Phys. **84**, 1253 (2012).

[47] R. Samanta, I. V. Protopopov, A. D. Mirlin, and D. B. Gutman, Phys. Rev. Lett. **122**, 206801 (2019).

[48] O. Narayan and S. Ramaswamy, Phys. Rev. Lett. **89**, 200601 (2002).

[49] H. Spohn, J. Stat. Phys. **154**, 1191 (2014).

[50] K. V. Samokhin, J. Phys.: Condens. Matter **10**, L533 (1998).

[51] The precise meaning and the value of the fermionic mass m in Eq. (7) may depend on the short-distance cutoff imposed on the Hamiltonian (1). It coincides with the bare electron mass, if the cutoff of the order of Fermi momentum is assumed, or may include some interaction-induced renormalization if the theory is regularized at smaller momenta.

[52] R. G. Pereira, J. Sirker, J.-S. Caux, R. Hagemans, J. M. Maillet, S. R. White, and I. Affleck, Phys. Rev. Lett. **96**, 257202 (2006).

[53] S. Lukyanov, Nucl. Phys. B **522**, 533 (1998).

[54] G. Refael and E. Altman, C. R. Phys. **14**, 725 (2013).

[55] V. Gurarie and J. T. Chalker, Phys. Rev. Lett. **89**, 136801 (2002).

[56] V. Gurarie and J. T. Chalker, Phys. Rev. B **68**, 134207 (2003).

[57] A. Amir, Y. Oreg, and Y. Imry, Europhys. Lett. **124**, 16001 (2018).

[58] Our model (2) is slightly more general than that of Refs. [39–41] as it generically allows for the disorder described by two independent random functions $K(x)$ and $v(x)$. In this form it also applies to many other physical systems including JJ chains, see Sec. II.

[59] E. Langmann and P. Moosavi, Phys. Rev. Lett. **122**, 020201 (2019).

[60] J. Lin, K. A. Matveev, and M. Pustilnik, Phys. Rev. Lett. **110**, 016401 (2013).

[61] A. Mirlin, Phys. Rep. **326**, 259 (2000).

[62] L. Pitaevskii and E. Lifshitz, *Physical Kinetics* (Elsevier Science, Amsterdam, 2012), Vol. 10.

[63] B. L. Altshuler, Y. Gefen, A. Kamenev, and L. S. Levitov, Phys. Rev. Lett. **78**, 2803 (1997).

[64] A. D. Mirlin and Y. V. Fyodorov, Phys. Rev. B **56**, 13393 (1997).

[65] An alternative derivation of the characteristic scale (31) was presented in Ref. [90].

[66] S. Banerjee and E. Altman, Phys. Rev. Lett. **116**, 116601 (2016).

[67] K. A. Matveev and Z. Ristivojevic, Phys. Rev. B **99**, 155428 (2019).

[68] S. Tarucha, T. Honda, and T. Saku, Solid State Commun. **94**, 413 (1995).

[69] A. Yacoby, H. L. Stormer, N. S. Wingreen, L. N. Pfeiffer, K. W. Baldwin, and K. W. West, Phys. Rev. Lett. **77**, 4612 (1996).

[70] B. E. Kane, G. R. Facer, A. S. Dzurak, N. E. Lumpkin, R. G. Clark, L. N. Pfeiffer, and K. W. West, Appl. Phys. Lett. **72**, 3506 (1998).

[71] O. M. Auslaender, A. Yacoby, R. de Picciotto, K. W. Baldwin, L. Pfeiffer, and K. West, Science **295**, 825 (2002).

[72] O. M. Auslaender, H. Steinberg, A. Yacoby, Y. Tserkovnyak, B. I. Halperin, K. W. Baldwin, and K. W. West, Science **308**, 88 (2005).

[73] H. Steinberg, G. Barak, A. Yacoby, L. N. Pfeiffer, K. W. West, B. I. Halperin, and K. L. Hur, Nat. Phys. **4**, 116 (2007).

[74] G. Barak, H. Steinberg, L. N. Pfeiffer, K. W. West, L. Glazman, F. von Oppen, and A. Yacoby, Nat. Phys. **6**, 489 (2010).

[75] C. P. Scheller, T.-M. Liu, G. Barak, A. Yacoby, L. N. Pfeiffer, K. W. West, and D. M. Zumbühl, Phys. Rev. Lett. **112**, 066801 (2014).

[76] J. A. Nixon and J. H. Davies, Phys. Rev. B **41**, 7929 (1990).

[77] J. A. Nixon, J. H. Davies, and H. U. Baranger, Phys. Rev. B **43**, 12638 (1991).

[78] A. Dhar, Phys. Rev. Lett. **86**, 5882 (2001).

[79] I. V. Gornyi, A. D. Mirlin, M. Müller, and D. G. Polyakov, Ann. Phys. **529**, 1600365 (2017).

[80] O. A. Castro-Alvaredo, B. Doyon, and T. Yoshimura, Phys. Rev. X **6**, 041065 (2016).

[81] B. Bertini, M. Collura, J. De Nardis, and M. Fagotti, Phys. Rev. Lett. **117**, 207201 (2016).

[82] J.-S. Caux, B. Doyon, J. Dubail, R. Konik, and T. Yoshimura, Sci. Post. Phys. **6**, 70 (2019).

[83] V. B. Bulchandani, R. Vasseur, C. Karrasch, and J. E. Moore, Phys. Rev. Lett. **119**, 220604 (2017).

[84] V. B. Bulchandani, R. Vasseur, C. Karrasch, and J. E. Moore, Phys. Rev. B **97**, 045407 (2018).

[85] J. D. Nardis, D. Bernard, and B. Doyon, Sci. Post. Phys. **6**, 49 (2019).

[86] S. Gopalakrishnan, R. Vasseur, and B. Ware, Proc. Natl. Acad. Sci. **116**, 16250 (2019).

[87] U. Agrawal, S. Gopalakrishnan, and R. Vasseur, Phys. Rev. B **99**, 174203 (2019).

[88] Equation (11) of Ref. [41] contains a typo: a missing factor of $1/n(x)$ in the first term.

[89] G. Rastelli, I. M. Pop, and F. W. J. Hekking, Phys. Rev. B **87**, 174513 (2013).

[90] M. Arzamasovs, F. Bovo, and D. M. Gangardt, Phys. Rev. Lett. **112**, 170602 (2014).